Journal of Luminescence 129 (2009) 376–381

Contents lists available at ScienceDirect

Journal of Luminescence

journal homepage: www.elsevier.com/locate/jlumin

Population inversion between the $^3H_4$ and the $^3F_4$ excited states of Tm^{3+} investigated by means of numerical solutions of the rate equations system in Tm^{3+}-doped and Tm^{3+}, Ho^{3+}-codoped fluoride glasses

A.F.H. Librantz [a], L. Gomes [b,*]

[a] Department of Sciences, UNINOVE, São Paulo, SP 02111-030, Brazil
[b] Center for Lasers and Applications, IPEN/CNEN-SP, P.O. Box 11049, São Paulo, SP 05422-970, Brazil

ARTICLE INFO

Article history:
Received 16 May 2008
Accepted 6 November 2008
Available online 19 November 2008

PACS:
78.50
78.55
71.55

Keywords:
1.5 μm-Laser emission
Energy-transfer constant rate
Numerical simulation
Rate equations system
Thulium-doped fluoride glass

ABSTRACT

Population inversion between the $^3H_4$ and the $^3F_4$ excited states of Tm^{3+} ions responsible for the 1.5 μm emission in Tm^{3+} singly doped (0.5%) and Tm^{3+}, Ho^{3+}-codoped fluoride (ZBLAN) glasses and its dependence on the Ho^{3+} concentration ($x = 0.2$–1%) was investigated by means of numerical solution of the rate equations system for continuous pumping at 797 nm. Mean lifetimes of donor and acceptor states were evaluated by using the integration method applied to the best fitting of fluorescence curves previously reported. Lifetime values were used to obtain the rate constants of all non-radiative energy-transfer processes involved and a complete set of rate equations better describing the observations was given. The rate equations were solved by numerical method and the population inversion between the $^3H_4$ and the $^3F_4$ excited states of Tm^{3+} was calculated to examine the beneficial effects on the gain associated with Ho^{3+} codoping. The results have shown that Tm^{3+} population inversion is reached only for high Ho^{3+}-codoping ($\geqslant 0.3$ mol%). Highest population inversion ($\sim 1.6 \times 10^{18}$ Tm^{3+} ions cm^{-3}) was obtained in Tm(0.5%), Ho(1%)-codoped (ZBLAN) pumped by 2.8 kW cm^{-2}. This population inversion density is ~6.4 times higher than that one observed in Tm:Tb:GLKZ, Tm:Tb:Ge–Ga–As–S–CsBr and Tm:Ho:Ge–Ga–As–S–CsBr for a similar pumping condition ($\sim 2.5 \times 10^{17}$ cm^{-3}). In addition, Tm(0.5%):Ho(1%):ZBLAN presents the highest population inversion that linearly increases with the pumping intensity; this behavior does not show saturation effect at least for the maximum intensity of 12 kW cm^{-2} employed. The use of 1 mol% of Ho^{3+}-codoping maximizes the potential gain of Tm^{3+}-doped (0.5%) ZBLAN to produce stimulated emission near 1.5 μm, making this material suitable for using it as fiber optical amplifier and/or fiber laser operating in 1.4–1.5 μm region of the spectrum.

1. Introduction

In the last years, Tm-doped glasses have been investigated for using as fiber lasers and optical amplifiers [1] based on the $^3H_4 \rightarrow {}^3F_4$-stimulated transition of Tm^{3+}. However, two intrinsic properties of Tm^{3+} single-doped materials act detrimentally, reducing its capacity of light signal amplification in S band (1.45–1.53 μm) in many oxide glasses, in which the $^3H_4$ level easily decay to the next lower-level $^3H_5$ via multiphonon relaxation. That is not the case of the fluorozirconate (ZBLAN) glass used in this work. Nevertheless, the lifetime of the lower $^3F_4$ level involved in the 1.47 μm emission is considerably longer than that of the upper $^3H_4$ level (~6 times is observed in Tm:ZBLAN and Tm:Ge–Ga–As–S–CsBr, and ~8.3 times in germanate glasses). To realize population inversion in Tm^{3+} ions, Ho^{3+} (0.15%) or Tb^{3+} (0.15%) ions have been used to codope the Tm-doped material to depopulate the $^3F_4$ level of Tm^{3+} in fluoroindate [2], fluorozirconate (ZBLAN) [3,4], fluorogermanate [5], tellurite [6] and chalcogenide [7] glasses. Because the energies of $^5I_7$ and $^7F_{0,1,2}$ levels of Ho^{3+} and Tb^{3+}, respectively, coincide with the energy of the $^3F_4$ level, holmium and terbium ions may actuate as deactivator of the $^3F_4$ lowest excited state of Tm^{3+} to improve the population inversion of Tm^{3+} ions in many luminescent solid materials. Besides the $^3H_4$ and $^3F_4$ fluorescence decay effects of Tm^{3+} caused by Ho^{3+} ions have been investigated in fluorozirconate [3] and more recently in fluorogermanate glass [5], a detailed investigation of the mechanisms of $^3H_4$ and $^3F_4$ deactivation are still lacking, as well the extension to high holmium doping effects. Also, a better approach of calculating the population inversion in Tm:Ho system needs to be performed based on the numerical solutions of a realistic set of rate equations, which can describe the system behavior under continuous pumping of the $^3H_4$ state. In this work, we investigated the population inversion of $^3H_4 \rightarrow {}^3F_4$

* Corresponding author. Tel.: +55 11 38169319; fax: +55 11 38169315.
E-mail addresses: librantz@uninove.br (A.F.H. Librantz), igomes@ipen.br (L. Gomes).

0022-2313/$ - see front matter © 2008 Elsevier B.V. All rights reserved.
doi:10.1016/j.jlumin.2008.11.002

transition of Tm^{3+} in Tm^{3+}-doped and Tm^{3+}, Ho^{3+}-codoped ZBLAN glasses due to its favorable optical properties such a wide transmission window (typically 300–5000 nm), good corrosion resistance and mechanical stability, and low cut-off phonon energy among glass materials (800 cm^{-1}). Also this material has high solubility for rare earth doping and low fusion temperature. A depopulation of $^3F_4$ state of Tm^{3+} by the energy transfer to Ho^{3+} ions is an important phenomena in solids that must be investigated among different host materials to establish a wide comparison of the physical effects in the upper and lower excited states of the $^3H_4 \rightarrow {}^3F_4$ transition to determine the best deactivator concentration to maximize the population inversion and consequently the gain for light signal amplification at 1.47 μm. This population inversion was calculated using the numerical solutions obtained using the Runge–Kutta method applied to the rate equations system. This method has been recently used to investigate the population inversion of $^3H_4 \rightarrow {}^3F_4$ transition of Tm^{3+} in Tm:Tb [4] and Tm:Eu:germanate [8] glasses giving an important contribution for understanding the potential and limitations of Tm^{3+} and Tm-doped materials for light signal amplification.

2. Experimental procedure

Best fitting parameters of $^3H_4$ excited level luminescence decay of Tm^{3+} (at 1470 nm) and best fitting energy-transfer parameters of $^5I_7$ (at 2000 nm) excited level luminescence transient of Ho^{3+}, previously reported for Tm:Ho:ZBLAN [3], were used in this work to obtain the mean lifetime by applying the integration method. The transfer rate constant was obtained using the mean lifetime value for each related energy-transfer process and it was used to solve the rate equations system to perform the population inversion investigation.

3. Results and discussion

Fig. 1 shows the simplified energy levels scheme used for the Tm:Ho:ZBLAN system used for continuous laser pumping of $^3H_4$ (Tm^{3+}) level (n_3) at 797 nm. The n_1, n_2 and n_3 represent the population of the $^3H_6$, $^3F_4$ and $^3H_4$ levels of Tm^{3+}, and n_4, n_5 and n_6 are the populations of $^5I_8$, $^5I_7$ and $^5I_6$ levels of Ho^{3+}, respectively.

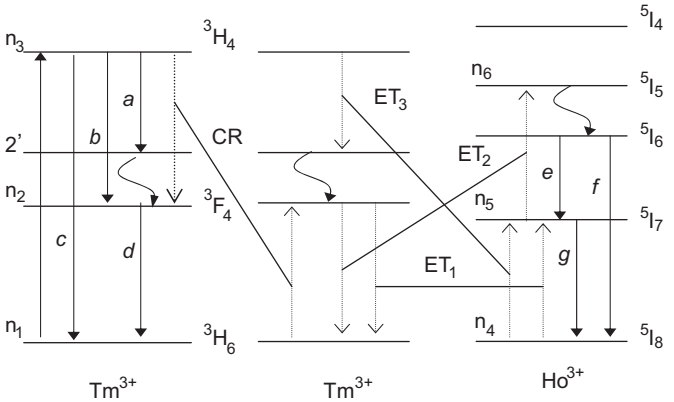

Fig. 1. A schematic energy levels diagram used for the Tm:Ho:ZBLAN considered for continuous laser pumping at 797 nm (solid up-arrow). n_1, n_2, n_3 represents the Tm^{3+} populations and n_4, n_5, n_6 are the Ho^{3+} populations. Radiative transitions are indicated as: $a = 2300$ nm, $b = 1470$ nm ($\beta_{32}+\beta_{32'} = 0.1$), $c = 800$ nm ($\beta_{31} = 0.9$), $d = 1800$ nm, $e = 2900$ nm, $f = 1200$ nm and $g = 2000$ nm.

3.1. Mean lifetime and energy-transfer rate constant determination

The following non-radiative energy-transfer (ET) processes (dipole–dipole interaction) were considered been involved in the optical cycle of Tm:Ho:ZBLAN under 797 nm excitation.

(i) $Tm^{3+}(^3H_4):Tm^{3+}(^3H_6) \rightarrow Tm^{3+}(^3F_4):Tm^{3+}(^3F_4)$—cross relaxation (CR);
(ii) $Tm^{3+}(^3F_4):Ho^{3+}(^5I_8) \rightarrow Tm^{3+}(^3H_6):Ho^{3+}(^5I_7)$—energy transfer ($ET_1$);
(iii) $Ho^{3+}(^5I_7):Tm^{3+}(^3H_6) \rightarrow Ho^{3+}(^5I_8):Tm^{3+}(^3F_4)$—back-transfer (BT);
(iv) $Tm^{3+}(^3F_4):Ho^{3+}(^5I_7) \rightarrow Tm^{3+}(^3H_6):Ho^{3+}(^5I_6)$—energy transfer ($ET_2$);
(v) $Tm^{3+}(^3H_4):Ho^{3+}(^5I_8) \rightarrow Tm^{3+}(^3H_5):Ho^{3+}(^5I_7)$—energy transfer ($ET_3$).

These ET processes have been previously investigated in Tm:Ho:ZBLAN glasses [3] by means of using a time-resolved luminescence technique and a tunable OPO laser excitation (1100–2000 nm). The luminescence decay of $^3H_4$ and $^3F_4$ excited states of Tm^{3+} in Tm:Ho:ZBLAN were best fitted by using a combination of the Inokuti–Hirayama function (transfer parameter γ) and a proposed localized interaction described by an exponential term with a decay rate K, according to Ref. [3]. Energy-transfer parameters γ and K were used to determine the mean lifetime of the donor ($^3H_4$) and acceptor ($^5I_7$) states.

The following equations have been used to fit the luminescence decay curves of Tm^{3+} at 1470 nm with short laser pulse of 4 ns (10 Hz) at 797 nm ($E \sim 10$ mJ) and Ho^{3+} luminescence transient (at 2000 nm) excited by $Tm^{3+}(^3F_4) \rightarrow Ho^{3+}(^5I_7)$ transfer induced by pulsed laser excitation at 1671 nm (4 ns, $E \sim 10$ mJ) [3].

(i) 1.47 μm-luminescence dec

$$I_D(t) = a\,\exp\left(-\frac{t}{\tau_D} - \gamma\sqrt{t}\right) + b\,\exp(-Kt) \quad (1)$$

(ii) 2 μm-luminescence transient:

$$I_A(t) = (a+b)\,\exp\left(-\frac{t}{\tau_A}\right) - \left[a\,\exp\left(-\frac{t}{\tau_D} - \gamma\sqrt{t}\right) + b\,\exp\left(-\frac{t}{\tau_D} - Kt\right)\right] \quad (2)$$

where $\tau_D = \tau_{D_3} = 1.46$ ms is the intrinsic lifetime of $^3H_4$ excited state of Tm^{3+} in Eq. (1). $\tau_D = \tau_{D_2} = 8.9$ ms is the intrinsic lifetime of donor $^3F_4$ state of Tm^{3+} and $\tau_A = \tau_{A_5} = 16.4$ ms is the intrinsic lifetime of the acceptor $^5I_7$ state of Ho^{3+} in Eq. (2). The fitting parameters γ and K are the Tm–Ho transfer parameters. a and b are non-dimensional parameters related to the Inokuti–Hirayama [9] and localized transfer contributions [3], respectively. The mean lifetime of $^3H_4$ and $^3F_4$ excited levels of Tm^{3+} represented by τ_3 and τ_2 were obtained by using the integration of normalized luminescence decay curves. For instance, τ_2 was better determined by integration of the raise-time component of the luminescence transient curve of $^5I_7$ level of Ho^{3+}—the acceptor state. The luminescence decay of $^5I_7$ level is exponential with a lifetime τ_5. τ_3 and τ_2 mean lifetimes were obtained using:

(i) 1.47 μm-luminescence decay integration:

$$\tau_3 = \frac{1}{(a+b)}\int_0^\infty \left\{a\,\exp\left(-\frac{t}{\tau_{D_3}} - \gamma\sqrt{t}\right) + b\,\exp(-Kt)\right\} dt \quad (3)$$

(ii) 2 μm-luminescence raise-time integration:

$$\tau_{risetime}(^5I_7) = \tau_2 = \frac{1}{(a+b)}\int_0^\infty \left\{ a\,\exp\left(-\frac{t}{\tau_{D_2}} - \gamma\sqrt{t}\right) + b\,\exp\left(-\frac{t}{\tau_{D_2}} - Kt\right)\right\} dt \quad (4)$$

W_{CR}, K_1, K_2 and K_3 transfer rate constant of CR, ET_1, ET_2 and ET_3 processes, respectively were obtained using

$$W_{CR} = \frac{1}{\tau_3} - \frac{1}{\tau_{D_3}} \quad (5)$$

$$K_1 = \frac{1}{\tau_2} - \frac{1}{\tau_{D_2}} \quad (6)$$

$$K_2 = \frac{1}{\tau_5} - \frac{1}{\tau_{D_5}} \quad (7)$$

$$K_3 = \frac{1}{\tau_3} - \frac{1}{\tau_{D_3}} - K_1 \quad (8)$$

Mean lifetimes values were obtained by applying the integration method described by Eqs. (3) and (4) using the transfer rate constants obtained by Eqs. (5)–(8)—mean lifetimes and transfer rate constants were given in Tables 1 and 2. Branching ratio of luminescence, radiative lifetime and intrinsic total lifetime of the two lowest excited states of Ho^{3+} and Tm^{3+} ions are given in Table 3. In spite of K_2 rate is expected to be dependent on the excitation density (Tm^{3+}) (because ET_2 process involves two excited states interaction), we observed K_2 rate slightly increasing for Tm^{3+} excitation density increase from 0.5×10^{18} to 2×10^{18} cm^{-3}. However, it becomes constant when the excitation density is $\geqslant 3\times10^{18}\,cm^{-3}$. The excitation density was estimated by measuring the mean energy of the laser pulse at 1671 nm and the excitation volume estimated to be $1.57\times10^{-2}\,cm^{-3}$. This result is similar to that one reported [10] for the energy transfer up-conversion (ETU) involving two excited Ho^{3+} ions in the $^5I_7$ level in Ho-doped ZBLAN [11]. This result justifies the use of K_2 values mentioned in Table 2 as a rate constant of ET_2 process in the rate equations system (*class* 1) for numerical simulation since higher excited Tm^{3+} ion densities ($N^*\sim10^{19}\,cm^{-3}$) are usually present in the system to have stimulated emission at 1.5 μm under cw operation.

Table 1
Experimental values of energy transfer parameters (γ and K) obtained from Ref. [3] for 1.47 μm luminescence of $^3H_4$ excited state of Tm^{3+} for two sets of Tm(y):Ho(x):ZBLAN.

Tm:Ho (mol%)		Transfer parameter (best fitting)					Transfer rates	
(y)	(x)	γ ($s^{-1/2}$)	K ($10^3\,s^{-1}$)	a	b	τ_3 (μs)	W_{CR} ($10^3\,s^{-1}$)	K_3 (s^{-1})
0.5	0	12.1	1.8	0.95	0.05	961	0.355	0
0.5	1	11.9	1.9	0.92	0.09	952	0.366	0
1	1	40.2	3.2	0.82	0.20	432	1.602	28
3	1	182	25.0	0.64	0.40	50.6	19.08	0
6	1	357	153.2	0.31	0.73	9.7	102.4	0
9	1	231	395.6	0.09	0.97	5.6	176.9	0
1	0.5	42.3	2.7	0.16	0.16	437	1.602	0
1	2	53.3	2.4	0.11	0.11	368	1.602	429
1	3	66.6	3.4	0.07	0.07	310	1.602	934
1	4	73.3	10.3	0.09	0.09	236	1.602	1941

a represents the fraction of Inokuti–Hirayama contribution and *b* a fraction of localized transfer contribution (transfer constant *K*). Mean lifetime τ_3 was obtained by integration of luminescence decay. $\tau_D\sim\tau_{R_3} = 1.46$ ms. W_{CR} is the cross-relaxation rate between the excited $^3H_4$ and the ground $^3H_6$ states of Tm^{3+} in ZBLAN.

Table 3
Branching ratio of luminescence, radiative lifetime and total lifetime (experimental) of Tm^{3+} and Ho^{3+} in ZBLAN (lifetime measurements done in low concentrations of ~0.15 mol%).

	Branching ratio (β)	Radiative lifetime (ms)	Total lifetime (ms)	Non-radiative decay (s^{-1})
Transition (Tm^{3+})				
$^3H_4\rightarrow{}^3H_6$	0.9	1.32	1.46	~0
$^3H_4\rightarrow{}^3F_4$	0.1			
$^3F_4\rightarrow{}^3H_6$	1	8.9	6.56	~0
Transition (Ho^{3+})				
$^5I_6\rightarrow{}^5I_8$	0.9	5.87	3.5	115
$^5I_6\rightarrow{}^5I_7$	0.1			
$^5I_7\rightarrow{}^5I_8$	1	12.6	16.4	~0
Tm: Ho (mol %) (y):(x)	K_1 (s^{-1})	K_2 (s^{-1})	K_3 (s^{-1})	
0.5:0.3	2550	0	4	
0.5:0.4	3355	0	8	
0.5:0.5	4295	0.013	14	
0.5:1	8456	0.09	71	
0.5:1.5	12617	0.26	188	
0.5:2	16778	0.6	371	

Values of K_1, K_2, K_3 obtained by inspection of best-fit curves of experimental rate constant (K_i) as a function of [Tm^{3+}] and [Ho^{3+}] concentrations measured for the Tm(0.5):Ho(x):ZBLAN samples. These K_i values were used in the numerical simulations of the rate equations system.
$\sigma = 2.8\times10^{-21}\,cm^2$ at 797 nm (absorption cross-section of $^3H_6\rightarrow{}^3H_4$ transition).

Table 2
Experimental values of energy transfer parameters (γ and K) obtained from Ref. [3] for 2 μm luminescence of $^5I_7$ excited state of Ho^{3+} for two sets of Tm(y):Ho(x):ZBLAN.

Tm:Ho (mol%)		Transfer parameters (best fitting)				Mean lifetimes (integration)		Transfer rates	
(y)	(x)	γ ($s^{-1/2}$)	K ($10^3\,s^{-1}$)	a	b	τ_2 (μs)	τ_5 (ms)	K_1 ($10^3\,s^{-1}$)	K_2 (s^{-1})
0.5	0	0	0	1	0	8900	–	0	0
0.5	1	111.6	412	0.84	0.22	128.9	16.4	7.65	0
1	1	151.4	308.8	0.83	0.18	71.2	16.4	13.93	0
3	1	281.2	162.8	0.77	0.27	21.3	12.4	46.84	19.7
6	1	275.3	221.9	0.34	0.70	12.2	4.8	81.85	147
9	1	223	316.3	0.21	0.85	11.1	2.0	89.97	439
1	0.5	140.9	127	0.82	0.24	82.2	13.8	12.05	0
1	2	215.7	184.3	0.53	0.49	25.4	15.4	39.25	3.9
1	3	280.6	289.7	0.38	0.64	11.5	15.8	86.84	2.3
1	4	281.0	389.9	0.27	0.76	8.8	12.5	113.14	19

a represents the fraction of Inokuti–Hirayama contribution and *b* a fraction of localized transfer contribution (transfer constant *K*). Mean lifetime τ_2 was obtained by integration of raise-time component of 2 μm-emission of $^5I_7$ acceptor state (Ho^{3+}).

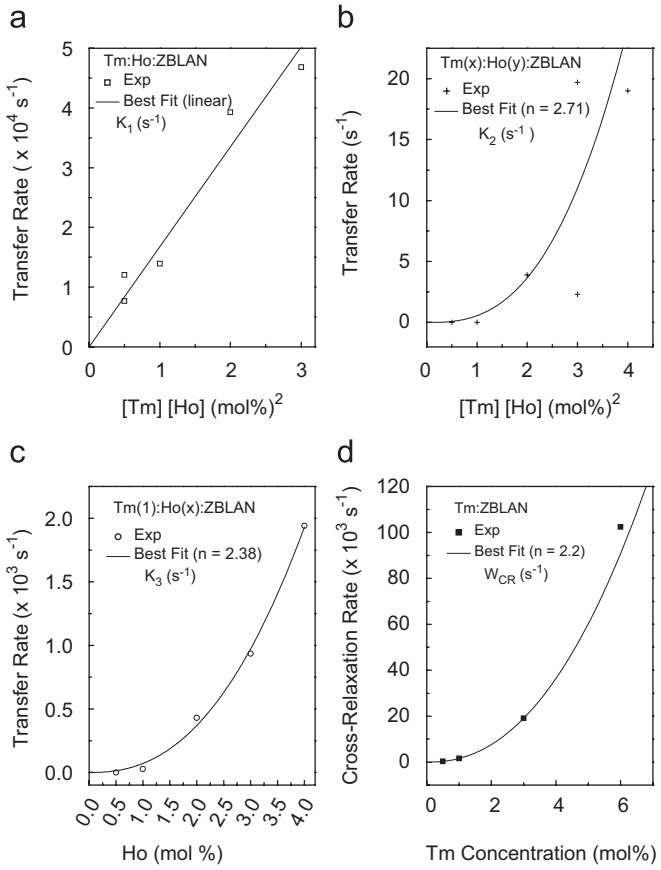

Fig. 2. Probability rate constants K_1, K_2 and K_3 (s^{-1}) due to Tm–Ho interactions as a function of [Tm^{3+}] [Ho^{3+}] concentrations product. (d) Tm–Tm cross-relaxation rate (W_{CR}) as a function of Tm^{3+} concentration.

Fig. 2(a) shows that K_1 has a linear dependence on ([Tm][Ho]) concentration, as is expected for a migration-assisted energy transfer involving excited donor and acceptor ions in the ground state. However, K_2 and K_3 exhibit non-linear concentration dependence, i.e., $K_2 \propto ([Tm][Ho])^{n=2.71}$ (see Fig. 2(b)) and $K_3 \propto [Ho]^{n=2.38}$ (see Fig. 2(c)), respectively. In addition, W_{CR} exhibits a quadratic dependence on Tm^{3+} concentration, $W_{CR} \propto [Tm]^{n=2.2}$, as expected for a cross-relaxation process (see Fig. 2(d)). Values of K_1, K_2, K_3 and W_{CR} rate constants were estimated for Tm(0.5%):Ho(*x*%) systems by inspecting the best-fitted curves shown in Figs. 2(a)–(d) and are listed in Table 3. These rate constants values were used in the numerical simulations performed in Section 3.3.

3.2. Rate equations for optical excitation of the $^3H_4$ level

Previous investigation of $^3H_4$ luminescence (~1470 nm) of Tm^{3+} in Tm:Ho:ZBLAN glass, excited by short laser pulses (4 ns) of 780 nm, has shown that a residual $^3F_4$ luminescence (~1800 nm) of ~20% remains besides the very strong $Tm(^3F_4) \rightarrow Ho(^5I_7)$ energy transfer [3]. In addition, this reminiscence luminescence of $^3F_4$ state exhibits an exponential decay with a lifetime similar to that one observed for single Tm-doped ZBLAN (~7 ms). On the other hand, residual $^3F_4$ luminescence was not observed in the case of Tm:Ho in tellurite [10], chalcogenide [7] and Tm:Tb in germanate (GLKZ) [4] glasses. This luminescence effect (residual) evidences that the fast energy migration through $^3F_4$ excited states leads to two distinct types of Tm^{3+} excited ions in ZBLAN glass (or classes): (i) *class* 1—excited Tm^{3+} ions close by Ho^{3+} that has a K_1 transfer rate resultant from $Tm(^3F_4) \rightarrow Ho(^5I_7)$ transfer minus $Ho(^5I_7) \rightarrow Tm(^3F_4)$ back-transfer rates and (ii) *class* 2—excited Tm^{3+} ions ($^3F_4$) far from Ho^{3+} ions (or isolated) having an intrinsic lifetime of ~7 ms. According to that observation, one can assume that 80% of Tm^{3+} ions interact with Ho^{3+} ions (*class* 1) and 20% behaves as

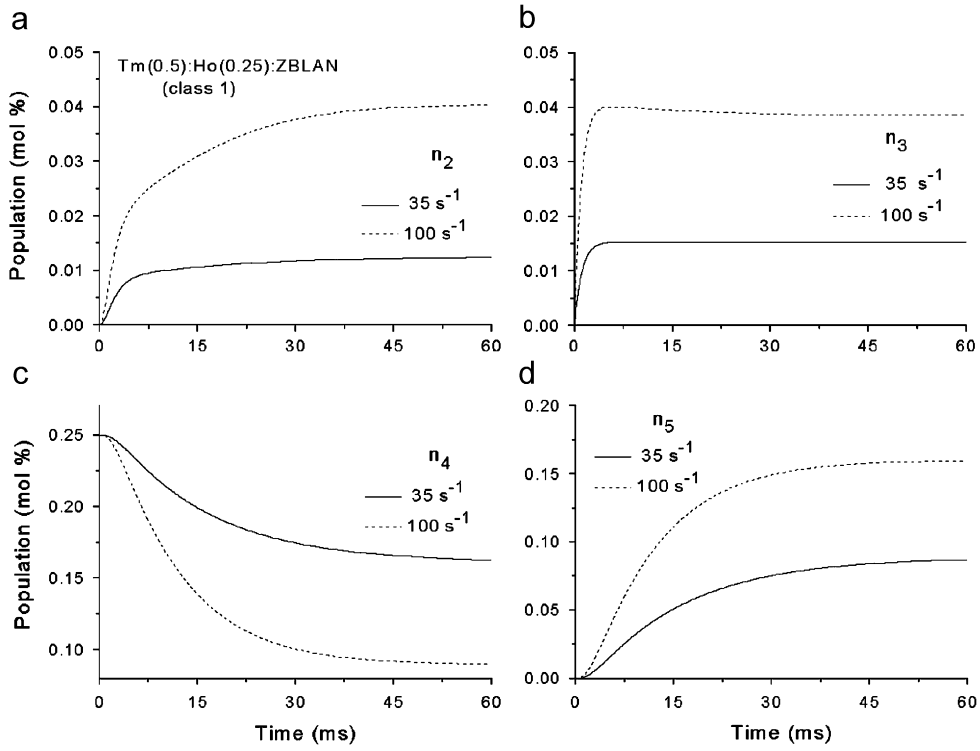

Fig. 3. Time evolution of $n_2(t)$ and $n_3(t)$ populations of Tm^{3+} and $n_4(t)$ and $n_5(t)$ populations of Ho^{3+}, numerical solutions of rate equations system (*class* 1) for Tm(0.5%):Ho(0.25%):ZBLAN continuous pumped at 797 nm. Pumping rates of 35 and 100 s^{-1} were used. Ho^{3+} ground state depopulation (n_4) precludes the population inversion (n_3–n_2<0) for higher pumping rate (100 s^{-1}) shown by dashed line of (c).

isolated Tm^{3+} ions (*class* 2). Based on this argument, we must have two distinct rate equations systems for Tm:Ho:ZBLAN glass. One set of rate equations for *class* 1 that includes ET_1, ET_2, ET_3 and CR processes and another set for *class* 2 (see rate equations system presented in Section 3.2).

Based on Fig. 1, one obtains the following rate equations system for the Tm:Ho:ZBLAN considered for continuous laser pumping the $^3H_4$ (Tm^{3+}) level (n_3) at 797 nm. The n_1, n_2 and n_3 represent the population of the $^3H_6$, $^3F_4$ and $^3H_4$ levels of Tm^{3+}, and n_4, n_5 and n_6 are the populations of the $^5I_8$, $^5I_7$ and $^5I_6$ levels of Ho^{3+}, respectively.

(i) Rate equations system for *class* 1:
In this case, it was used $n_1+n_2+n_3=n_{Tm}$ and $n_4+n_5+n_6=n_{Ho}$, where n_{Tm} and n_{Ho} are the Tm^{3+} and Ho^{3+} concentrations given in mol%:

$$\frac{dn_1}{dt} = -R_P n_1 + \frac{B_{21}}{\tau_{R_2}} n_2 + \frac{B_{31}}{\tau_{R_3}} n_3 - W_{CR} n_1 n_3 + K_1 n_2 n_4 + K_2 n_2 n_5 - K_{BT} n_1 n_5 \quad (9)$$

$$\frac{dn_2}{dt} = 2W_{CR} n_1 n_3 + \left(\frac{B_{32}}{\tau_{R_3}} + W_{nR}(32)\right) n_3 - \frac{\beta_{21}}{\tau_{R_2}} n_2 - K_1 n_2 n_4 - K_2 n_2 n_5 + K_3 n_3 n_4 \quad (10)$$

$$\frac{dn_3}{dt} = R_P n_1 - W_{CR} n_1 n_3 - \left(\frac{(\beta_{32''} + \beta_{32} + \beta_{31})}{\tau_{R_3}} + W_{nR}(32)\right) n_3 - K_3 n_3 n_4 \quad (11)$$

$$\frac{dn_4}{dt} = -K_1 n_2 n_4 + \frac{\beta_{64}}{\tau_{R_6}} n_6 + \frac{\beta_{54}}{\tau_{R_5}} n_5 - K_3 n_3 n_4 + K_{BT} n_1 n_5 \quad (12)$$

$$\frac{dn_5}{dt} = K_1 n_2 n_4 - \frac{\beta_{54}}{\tau_{R5}} n_5 + \left(\frac{\beta_{65}}{\tau_{R_6}} + W_{nR}(65)\right) n_6 + K_3 n_3 n_4 - K_2 n_2 n_5 - K_{BT} n_1 n_5 \quad (13)$$

$$\frac{dn_6}{dt} = K_2 n_2 n_5 - \left(\frac{(\beta_{65} + \beta_{64})}{\tau_{R_6}} + W_{nR}(65)\right) n_6 \quad (14)$$

(ii) Rate equations system for *class* 2:
In this case, it was used $n_1+n_2+n_3=n_{Tm}$.

$$\frac{dn_1}{dt} = -R_P n_1 + \frac{B_{21}}{\tau_{R_2}} n_2 + \frac{B_{31}}{\tau_{R_3}} n_3 - W_{CR} n_1 n_3 \quad (15)$$

$$\frac{dn_2}{dt} = 2W_{CR} n_1 n_3 + \left(\frac{B_{32}}{\tau_{R_3}} + W_{nR}(32)\right) n_3 - \frac{\beta_{21}}{\tau_{R_2}} n_2 \quad (16)$$

$$\frac{dn_3}{dt} = R_P n_1 - W_{CR} n_1 n_3 - \left(\frac{(\beta_{32''} + \beta_{32} + \beta_{31})}{\tau_{R_3}} + W_{nR}(32)\right) n_3 \quad (17)$$

$R_P = \sigma_{13} n_1 (I_P/h\nu)$ is the pumping rate (s^{-1}), I_P is the intensity of pumping given in ($W\,cm^{-2}$) and $h\nu$ is the photon energy of pumping radiation. β_{ij} represents the luminescence branching ratio and τ_{R_i} is the radiative lifetime of $^5I_6$, $^5I_7$ (Ho^{3+}) and $^3H_4$, $^3F_4$ (Tm^{3+}) excited states labeled as level $i=6, 5$ for Ho^{3+} and $i=3, 2$ (Tm^{3+}).

3.3. Numerical solution of the rate equations

Rate equations system was solved based on the Runge–Kutta numerical method of fourth order by means of a program developed in Scilab language. Tm^{3+} and Ho^{3+} populations were determined for Tm(0.5%):Ho(*x*%):ZBLAN system using the numerical solutions obtained for simulating a cw laser pumping at 797 nm. The Tm^{3+} and Ho^{3+} populations were obtained after the populations get the equilibrium (after ~80 ms). Tm^{3+} populations were obtained by considering the population distribution of *classes* 1 and 2, according to $n_i = 0.8n_i(1) + 0.2n_i(2)$ where $i=1, 2$ and 3. The Tm^{3+} population inversion was obtained using $\Delta n = n_3 - n_2$.

Fig. 3 shows the time evolution $n_2(t)$ and $n_3(t)$ populations of Tm^{3+} and $n_4(t)$ and $n_5(t)$ (Ho^{3+}) for a pumping rates of 35 and 100 s^{-1} after cw laser pumping at 797 nm. Looking the population values of Figs. 3(a) and (b) at $t=60$ ms, one can see that the pumping rate of 35 s^{-1} produces a population inversion (n_3–n_2) of 4.8×10^{17} cm^{-3} (*class* 1) in Tm(0.5%):Ho(0.25%) system. A negative population inversion was observed by increasing the pumping rate to 100 s^{-1}, as a consequence of the $Tm(^3F_4)\rightarrow Ho(^5I_7)$ transfer saturation induced by severe Ho^{3+} ground state depopulation. By comparing Fig. 3(c) and (d) one concludes that n_2 population increases at expenses of n_4 population—ground state of Ho^{3+}. The saturation effect of $Tm\rightarrow Ho$ transfer might be observed to happen for some high pumping rate (>100 s^{-1}) in more [Ho^{3+}] concentrated system (>0.3 mol%) (Fig. 4). Fig. 5 shows the population

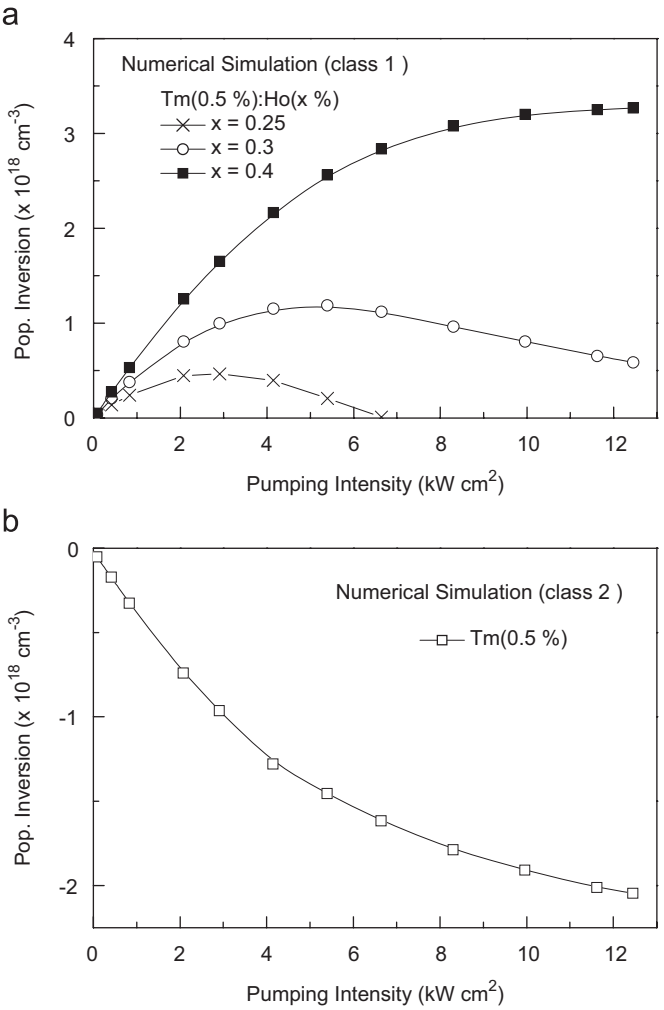

Fig. 4. The population density difference (n_3–n_2) obtained from numerical solutions of the rate equations system applied to Tm(0.5%):Ho(*x*%) system is shown as a function of the pumping intensity at 797 nm. (a) The result of numerical simulation applied to Tm–Ho system of *class* 1 for many [Ho^{3+}] concentrations, where $x=0.25$, 0.3 and 1 mol%. (b) The result applied to Tm(0.5%) system of *class* 2.

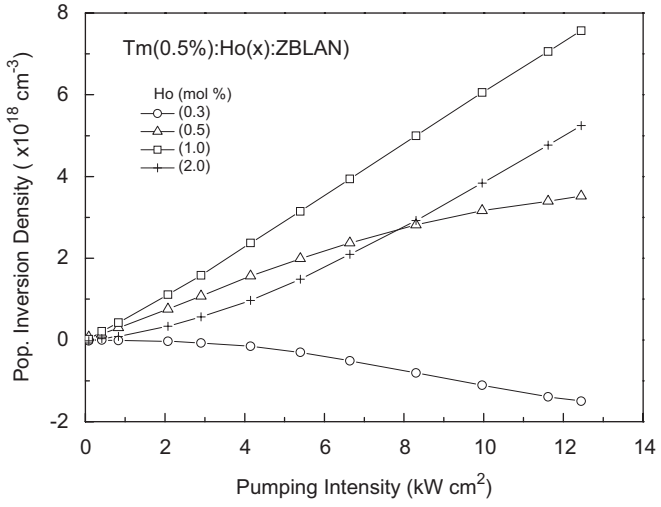

Fig. 5. It is shown the population density difference (n_3-n_2) obtained using the numerical solutions of rate equations system for Tm(0.5%):Ho(x%) system as a function of cw pumping intensity at 797 nm, for many Ho^{3+} concentrations, where $x = 0.3$, 0.5, 1 and 2 mol%.

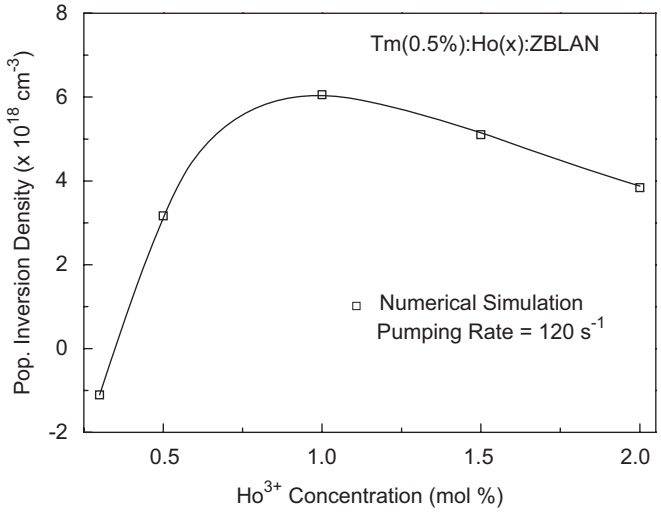

Fig. 6. Results of population density difference (n_3-n_2) obtained by numerical simulations applied to Tm(0.5%):Ho(x%) system for a constant pumping intensity of 10 kW cm^{-2} (or pumping rate of 120 s^{-1}) at 797 nm, for many Ho^{3+} concentrations (where $x = 0.3$, 0.5, 1, 1.5 and 2 mol%).

density difference (n_3-n_2) obtained using the numerical solutions of the rate equations system of Tm(0.5%):Ho(x):ZBLAN as a function of the pumping intensity at 797 nm performed for many Ho^{3+} concentrations, where $x = 0.5$, 1 and 2 mol%. Fig. 5 (open squares) shows a population inversion (n_3-n_2) that linearly increases on increasing the pumping intensity for [Ho^{3+}] concentration equal to 1 mol%, at least for the highest intensity of 12 kW cm^2 investigated. Fig. 6 shows that the population inversion (n_3-n_2) is maximized for 1 mol% of Ho^{3+} in Tm(0.5):Ho(x): ZBLAN for a constant pumping intensity of 10 kW cm^{-2}.

4. Conclusions

In this work, we investigated the population inversion in Tm(0.5%):Ho(x%):ZBLAN under continuous pumping at 797 nm for using it as optical amplifiers operating near 1.5 μm. Highest population inversion of Tm^{3+} was obtained using 1 mol% of Ho^{3+}. A population inversion density of 1.6×10^{18} Tm^{3+} ions cm^{-3} was obtained for a pump intensity of 2.7 kW cm^{-2}, which is ~5.3 times bigger that one verified in Tm(0.1%):Ho(0.15%):Ge–Ga–As–S–CsBr [7] (~3×10^{17} cm^{-3}). This population inversion density is also higher than that one estimated for Tm(0.1%):Tb(0.2%):GLKZ [4] (~2×10^{17} cm^{-3}) and for Tm(0.1%):Tb(0.15%):Ge–Ga–As–S–CsBr [7] (~2.5×10^{17} cm^{-3}) glasses for similar pumping conditions. This result points that Tm:Ho:ZBLAN doped with 0.5 mol% of Tm^{3+} and codoped with 1 mol% of Ho^{3+} maximizes its amplification potential gain based on the Tm^{3+}-stimulated emission near 1.5 μm, so making this material very promising system for light signal amplification in S-band of telecommunication.

Acknowledgment

The authors thank the financial support from FAPESP (Grants nos. 1995/4166-0 and 2000/1086-0) and CNPq.

References

[1] E.R.M. Taylor, L.N.Ng.J. Nilsson, R. Caponi, A. Pagano, M. Potenza, S. Sordo, IEEE Photon. Technol. Lett. 16 (3) (2004) 777;
E.R. Taylor, L.N. Ng, N.P. Sessions, H. Buerger, J. Appl. Phys. 92 (1) (2002) 112.
[2] W. Ryba-Romanowski, S. Golab, G. Dominiak-Dzik, M. Zelechower, J. Gabrys-Pisarska, J. Alloys Compds. 325 (2001) 215.
[3] L.D. da Vila, L. Gomes, L.V.G. Tarelho, S.J.L. Ribeiro, Y. Messaddeq, J. Appl. Phys. 95 (10) (2004) 5451.
[4] A.F.H. Librantz, L. Gomes, G. Pairier, S.J.L. Ribeiro, Y. Messaddeq, J. Lumin. 128 (2008) 51.
[5] L.A. Bueno, A.S.L. Gomes, Y. Messaddeq, C.V. Santilli, J. Dexpert-Ghys, S.J.L. Ribeiro, J. Non-Cryst. Solids 351 (2005) 1743.
[6] L.D. da Vila, L. Gomes, C.R. Eyzaguirre, E. Rodriguez, C.L. César, L.C. Barbosa, Opt. Mater. 27 (2005) 1333.
[7] J.H. Song, J. Heo, S.H. Park, J. Appl. Phys. 97 (2005) 083542.
[8] A.F.H. Librantz, L. Gomes, G. Pairier, S.J.L. Ribeiro, Y. Messaddeq, in: Proceedings of the SPIE, USA, 6190 (2006) G-1.
[9] M. Inokuti, H. Hirayama, J. Chem. Phys. 43 (6) (1965) 1978.
[10] L.D. da Vila, L. Gomes, C.R. Eyzaguirre, E. Rodriguez, C.L. César, L.C. Barbosa, Opt. Mater. 27 (2005) 1333.
[11] A.F.H. Librantz, S.D. Jackson, F.H. Jagosich, L. Gomes, G. Poirier, S.J.L. Ribeiro, Y. Messaddeq, J. Appl. Phys. 101 (2007) 123111.